

**UCC Library and UCC researchers have made this item openly available.
Please [let us know](#) how this has helped you. Thanks!**

Title	Resonant photoluminescence studies of carrier localisation in c-plane InGaN/GaN quantum well structures
Author(s)	Blenkhorn, William; Schulz, Stefan; Tanner, Daniel; Oliver, Rachel; Kappers, M. J.; Humphreys, C. J.; Dawson, Philip
Publication date	2018-03-20
Original citation	Blenkhorn, W., Schulz, S., Tanner, D., Oliver, R., Kappers, M. J., Humphreys, C. J. and Dawson, P. (2018) Journal of Physics: Condensed Matter, In Press, doi: 10.1088/1361-648X/aab818
Type of publication	Article (peer-reviewed)
Link to publisher's version	http://iopscience.iop.org/article/10.1088/1361-648X/aab818 http://dx.doi.org/10.1088/1361-648X/aab818 Access to the full text of the published version may require a subscription.
Rights	© 2018 IOP Publishing Ltd. This is an author-created, un-copyedited version of an article accepted for publication in Journal of Physics: Condensed Matter. The publisher is not responsible for any errors or omissions in this version of the manuscript or any version derived from it. The Version of Record is available online at http://iopscience.iop.org/10.1088/1361-648X/aab818 . As the Version of Record of this article is going to be published on a subscription basis, this Accepted Manuscript will be available for reuse under a CC BY-NC-ND 3.0 licence after a 12 month embargo period. https://creativecommons.org/licenses/by-nc-nd/3.0/
Embargo information	Access to this article is restricted until 12 months after publication by request of the publisher.
Embargo lift date	2019-03-20
Item downloaded from	http://hdl.handle.net/10468/5726

Downloaded on 2021-11-28T11:45:20Z

ACCEPTED MANUSCRIPT

Resonant photoluminescence studies of carrier localisation in c-plane InGaN/GaN quantum well structures

To cite this article before publication: William Blenkhorn *et al* 2018 *J. Phys.: Condens. Matter* in press <https://doi.org/10.1088/1361-648X/aab818>

Manuscript version: Accepted Manuscript

Accepted Manuscript is “the version of the article accepted for publication including all changes made as a result of the peer review process, and which may also include the addition to the article by IOP Publishing of a header, an article ID, a cover sheet and/or an ‘Accepted Manuscript’ watermark, but excluding any other editing, typesetting or other changes made by IOP Publishing and/or its licensors”

This Accepted Manuscript is © 2018 IOP Publishing Ltd.

During the embargo period (the 12 month period from the publication of the Version of Record of this article), the Accepted Manuscript is fully protected by copyright and cannot be reused or reposted elsewhere.

As the Version of Record of this article is going to be / has been published on a subscription basis, this Accepted Manuscript is available for reuse under a CC BY-NC-ND 3.0 licence after the 12 month embargo period.

After the embargo period, everyone is permitted to use copy and redistribute this article for non-commercial purposes only, provided that they adhere to all the terms of the licence <https://creativecommons.org/licenses/by-nc-nd/3.0>

Although reasonable endeavours have been taken to obtain all necessary permissions from third parties to include their copyrighted content within this article, their full citation and copyright line may not be present in this Accepted Manuscript version. Before using any content from this article, please refer to the Version of Record on IOPscience once published for full citation and copyright details, as permissions will likely be required. All third party content is fully copyright protected, unless specifically stated otherwise in the figure caption in the Version of Record.

View the [article online](#) for updates and enhancements.

1
2
3 Resonant photoluminescence studies of carrier localisation in c-plane InGaN/GaN quantum
4 well structures
5
6
7

8 W. E. Blenkhorn¹, S. Schulz², D. S. P. Tanner^{2,3}, R. A. Oliver⁴, M. J. Kappers⁴, C. J.
9 Humphreys⁴ and P. Dawson¹
10
11
12

13
14 ¹*School of Physics and Astronomy, Photon Science Institute, University of Manchester, M13*
15
16 *9PL, Manchester, UK*
17
18

19 ²*Photonics Theory Group, Tyndall National Institute, Dyke Parade, Cork, Ireland*
20
21

22 ³*Department of Physics, University College Cork, Cork, Ireland*
23
24

25 ⁴*Department of Material Science and Metallurgy, 27 Charles Babbage Road, University of*
26
27 *Cambridge, Cambridge, CB3 0FS, UK*
28
29

30
31 **Abstract**
32

33
34 In this paper we report on changes in the form of the low temperature (12K)
35 photoluminescence spectra of an InGaN/GaN quantum well structure as a function of
36 excitation photon energy. As the photon energy is progressively reduced we observe at a
37 critical energy a change in the form of the spectra from one which is determined by the
38 occupation of the complete distribution of hole localisation centres to one which is
39 determined by the resonant excitation of specific localisations sites. This change is governed
40 by an effective mobility edge whereby the photo-excited holes remain localised at their initial
41 energy and are prevented from scattering to other localisation sites. This assignment is
42 confirmed by the results of atomistic tight binding calculations which show that the wave
43 function overlap of the lowest lying localised holes with other hole states is low compared
44 with the overlap of higher lying hole states with other higher lying hole states.
45
46
47
48
49
50
51
52
53
54
55
56
57
58
59
60

Introduction

The nature of the radiative recombination process(es) in InGaN/GaN quantum wells (QWs) has been extensively investigated since the pioneering work of Akasaki, Amano and Nakamura [1] demonstrated the potential that the InGaN materials system has for producing optoelectronic devices that emit in the near UV through the visible part of the spectrum. One of the main reasons for this analysis is that the room temperature internal quantum efficiency of light emitting diodes can be very high, despite the presence of extended defects with densities $\sim 10^8 \text{ cm}^{-2}$. The most commonly accepted explanation is that the local microstructure of the QWs leads to localisation that prevents carrier diffusion to non-radiative centres. The outstanding questions related to the localisation have concerned the nature of the localisation centres. Probably the most significant step forward in this area was the demonstration by Galtrey et al [2] that the In atoms were distributed randomly in c-plane structures and that previous reports [3,4] of In clustering which was believed to be the cause of carrier localisation could be an artefact of the measurement technique used [5]. Indeed further evidence has emerged that the In atoms in InGaN QWs grown in our laboratory are randomly distributed as has been described by Bennett et al [6] and Tang et al [7]. Along with the suggestion by Graham et al [8] that well width fluctuations could be more effective for localising carriers than previously thought, led to significant reappraisals of the overall energy landscape in InGaN/GaN QWs.

Distinct theoretical approaches by Watson-Parris et al [9] who used an effective mass treatment and Schulz et al [10] who applied an atomistic tight binding model both led to the following overall picture of c-plane InGaN/GaN QWs: in the situation where In atoms are randomly distributed they can be very effective at localising holes whereas electrons are more likely to be localised at well width fluctuations. Schulz et al [10] also found that the spatial separation of the electron and hole wave functions due to the presence of the built-in potential

1
2
3 leads to a relatively weak electron-hole Coulomb interaction so that localised electrons and
4
5 holes can be considered as independent. The results of both theoretical approaches are
6
7 supported by the experimental data where it was found that the low temperature
8
9 photoluminescence (PL) line widths (ignoring phonon effects) were very similar to the
10
11 calculations of fluctuations in the hole localisation energies. Additionally, one factor which is
12
13 not explicitly considered in our model is the incorporation of indium into the gallium nitride
14
15 barrier, which is known to affect the calculated electron and hole energies in continuum
16
17 models. In general, in our atomistic description the well barrier interface is not as sharp as in
18
19 a continuum based description. This originates from the fact that the atomic arrangement of
20
21 In atoms at the well barrier interfaces varies locally. We note that a more realistic indium
22
23 profile across the quantum well interface was included in our earlier theoretical studies using
24
25 a modified continuum model [9]. Where the modified continuum model (with the indium
26
27 penetration into the barrier) and our current atomistic model (without such indium penetration
28
29 into the barrier) address the same questions, they give very similar results, suggesting that the
30
31 non-sharp interface is not the key factor influencing the carrier localisation. It should be
32
33 stressed that in the above we are only referring to the energetically low lying localised
34
35 electron and hole states. The effects of carrier localisation also manifest themselves in the
36
37 anomalous temperature dependence of the peak PL energy [11] and the form of the low
38
39 temperature PL decay curves [12,13]. To gain insight into impact of alloy fluctuations in
40
41 InGaN/GaN QWs from theory different approaches have been applied. These methods range
42
43 from localization landscape theory [14][15], modified continuum-based models [9] and
44
45 atomistic tight-binding calculations [10].
46
47
48
49
50
51
52
53

54 Carrier localisation in semiconductor systems has been widely studied and has proved
55
56 particularly amenable to optical studies where the photon energy of the excitation is resonant
57
58 with either specific features in the absorption or excitation spectrum [16,17] or with the
59
60

1
2
3 conventional emission spectrum [18,19]. Somewhat surprisingly the use of resonant
4 spectroscopy has not been widespread in the study of InGaN/GaN QWs but the technique has
5
6 been used by Satake et al [20], Schmidt et al [21], Graham et al [22] and Hylton et al [23]. Of
7
8 particular relevance to the work reported here is the previous study [18] where it was
9
10 observed that at low temperatures as the excitation photon energy was reduced below some
11
12 critical value the peak PL shifted to lower energy. The onset of this shift was attributed to
13
14 excitation below a mobility edge [24] that prevented all the localised states being occupied. It
15
16 should be noted that the observation of a mobility edge in InGaN/GaN QWs has also been
17
18 reported using pump-probe spectroscopy [25].
19
20
21
22
23

24
25 In this paper we extend our previous work [22] and study the form of the PL spectrum from a
26
27 c-plane InGaN/GaN structure at low temperature as a function of excitation energy and
28
29 correlate the results with atomistic calculations [26] of the ground and excited localised states
30
31 of electrons and holes. At $T=12\text{K}$ for excitation photon energies above a certain critical
32
33 energy the form of PL spectrum reflects the random occupation of the localised hole states
34
35 but for photon energies below this critical energy the form of the spectrum reflects the fact
36
37 that the holes remain localised in the states in which they are resonantly excited. We interpret
38
39 the critical energy as being due to a mobility edge whereby the holes cannot scatter to lower
40
41 lying hole states. The growth of InGaN QWs on sapphire leads to very large defect densities,
42
43 indeed in the sample reported on here the defect density is $< 3 - 6 \times 10^8 \text{ cm}^{-2}$. Nevertheless
44
45 we do not believe these defects influence our conclusions as the work was performed at 12K
46
47 where the effects of defects are negated by localisation, indeed we have demonstrated
48
49 previously [27] that the internal quantum efficiency in similar structures both at low and high
50
51 temperatures are independent of defects for densities $< 10^9 \text{ cm}^{-2}$. Also we note that the
52
53 majority of commercial LEDs are grown on such highly defective substrates and our study is
54
55 thus relevant to the majority of material grown today.
56
57
58
59
60

Methods

A 10 period $\text{In}_{0.17}\text{Ga}_{0.83}\text{N}$ (2.5 nm)/GaN (7.3 nm) QW structure was grown by metal organic vapour-phase epitaxy in a Thomas Swan 6 x 2 inch close-coupled showerhead reactor. The structure was grown on low defect density c-plane sapphire/GaN pseudo-substrates on c-plane sapphire with a nominal 0.25° miscut toward (11-20). The QWs were grown using a Q2T methodology [28] where following the growth of the QW at 756°C a 1 nm thick GaN QW cap was grown. The temperature was then ramped up to 860°C and then the rest of the barrier was grown. The sample was mounted in a closed cycle cryostat at Brewster's angle to minimise the effects of interference fringes [22]. The PL was excited by chopped light from a tuneable dye laser at an excitation power density of 250 Wcm^{-2} . The PL was dispersed by a 0.85 m double grating spectrometer and detected by a GaAs photomultiplier whose output was processed by a lock-in detector. It should be noted that the same results as reported here were also obtained on a sample grown using a 2T growth methodology [28] which leads to gross fluctuations in the QW width on a lateral scale of 50 to 100 nm. This implies that the microstructure on a lateral scale smaller than that of the gross well width fluctuations is controlling this aspect of the optical properties.

Results and Discussion

In figure 1 are shown PL spectra at a temperature of $T=12\text{K}$ when exciting the sample with light of photon energies of 2.973 eV and 2.783 eV. The PL spectrum excited by light with the greater photon energy consists of a main recombination with peak energy of 2.774 eV and a weaker feature with peak energy of 2.684 eV. These are identified [8] as being due to recombination involving localised electrons and holes (2.774 eV) and LO phonon assisted (2.684 eV) recombination of the main PL peak. It should be noted that the form of PL spectrum remains unchanged when the excitation photon energy is greater than 2.812 eV; we

1
2
3 refer to spectra taken under this set of conditions as non-resonant PL. When the excitation
4 photon energy was reduced to 2.783 eV in figure 1 the PL spectrum is changed radically. In
5 this particular case the excitation photon energy lies within the non-resonant PL spectrum as
6 indicated by the red arrow, this we refer to as *resonant excitation*. As discussed by Graham et
7 al [22], following the work by Cohen et al [18] and Permogorov et al [19], the features A
8 (2.753 eV), B (2.690 eV) and C (2.663 eV) are identified as follows. Feature A is ascribed to
9 acoustic phonon assisted absorption and recombination of the directly excited localised
10 electrons and holes at the excitation photon energy, feature B is due to emission from the
11 resonantly excited states which are accompanied by the emission of an LO phonon with
12 feature C being the LO phonon replica of feature A.
13
14
15
16
17
18
19
20
21
22
23
24
25
26

27 In figure 2 are shown low temperature PL spectra as the excitation photon energy is moved
28 across the non-resonant PL spectrum. Once the excitation photon energy is less than 2.812
29 eV, the peaks A, B, C (as defined in figure 1) all move by equal amounts to lower energy
30 reflecting the specific excitation of a subset of the localised electrons and/or holes with the
31 excitation photon energy used. So for excitation photon energies above 2.812 eV the form of
32 the spectra remain unchanged but for excitation photon energies below 2.812 eV the spectral
33 peaks move to lower energy with decreasing excitation photon energy. This behaviour is
34 reflected in the graph in figure 3. We interpret this behaviour in terms of a mobility edge,
35 which defines the critical energy below which photo excited carriers cannot occupy the full
36 distribution of localised states. To fully understand this behaviour we need to have
37 information on the available energy states for both electrons and holes.
38
39
40
41
42
43
44
45
46
47
48
49
50
51
52

53 To understand this behaviour, we have applied the atomistic tight-binding model described in
54 refs [10] and [26] to study the electron and hole states of c-plane InGaN/GaN QWs. In this
55 approach we account for well width and random alloy fluctuations. The strain and built-in
56 field variations arising from random alloy fluctuations are treated on a microscopic level by
57
58
59
60

1
2
3 using valence force field and local polarization methods. Within this framework we have
4 modelled a c-plane $\text{In}_{0.15}\text{Ga}_{0.85}\text{N}/\text{GaN}$ QW with a width of approximately 3 nm. We note that
5
6 whereas our calculations were performed for a QW thickness of 3nm, the measured thickness
7
8 was 2.5nm. Since the key point for understanding the data is the detailed description of both
9
10 ground and localized hole states, the well width is of secondary importance for the
11
12 conclusions drawn here. Our main focus is on carrier localization and how this feature
13
14 changes with energy. It is beyond the scope of the present study to match, for instance,
15
16 transition energies, where the well width will play a role. In the present work, it is more
17
18 important that quantities such as the FWHM are reasonably described (as they are) by our
19
20 model, since this gives an indication of the energy distribution of localized states. The
21
22 calculations have been performed on $\approx 82,000$ atom supercells (equivalent to a system size of
23
24 10 nm x 9 nm x 10 nm) with periodic boundary conditions. 175 configurations have been
25
26 used to obtain reliable statistical averages and thus to compare our results with the
27
28 experimental data. For instance, when calculating the PL emission spectra we find a full
29
30 width of half maximum (FWHM) value of $\text{FWHM}^{\text{theo}} = 84$ meV which is in reasonable
31
32 agreement with the experimental data of $\text{FWHM}^{\text{exp}} = 65$ meV. A detailed discussion of the
33
34 factors that influence the calculated FWHM is given in our previous work [26] where we
35
36 noted that the interplay of well width fluctuation and built-in field can affect the variation of
37
38 the electron ground state energy as a function of the microscopically different configurations.
39
40 In turn, this can lead to the situation that the calculated FWHM values are larger when
41
42 compared to the experiment. In general, all this is affected by statistical fluctuations in the
43
44 size and shape of well width fluctuations and the connected changes in the electronic
45
46 structure of the system. Given that we have a reasonably good agreement between theory and
47
48 experiment for the FWHM, and therefore the energy distribution of the localized states, the
49
50 agreement between theory and experiment is sufficient for the present work, where we are
51
52
53
54
55
56
57
58
59
60

interested in factors that influence the observation of the mobility edge. Thus the chosen number of configurations is sufficient to obtain a good description of the energy variation in electron and hole states originating from random alloy fluctuations, which is key to understanding the experimental findings. Central to the existence of a mobility edge is the ability of carriers to transfer from a state of a given energy to another state with a different energy. Moreover, in this context the question is if there is any major difference between electron and hole states. To shed light on this question we have calculated the modulus overlap $\Omega_{nm}^\lambda = \sum_i^N |\psi_{n,i}^\lambda| |\psi_{m,j}^\lambda|$, between the states ψ_m^λ and ψ_n^λ , for electrons ($\lambda = e$) and holes ($\lambda = h$). The index i denotes the lattice site in the atomistic grid. For each of the 175 configurations, the calculation of Ω_{nm}^e has been performed for 5 electron states; for the holes 40 states have been taken into account to calculate Ω_{nm}^h . To achieve an energy resolved distribution of Ω_{nm}^λ for electrons and holes using the different microscopic configurations, overlaps for given states/energies have been grouped together in energy bins of the width of 30 meV and 20 meV for electrons and holes, respectively. The difference in the bin size accounts for difference in the localization features of electrons and holes. Overlaps in each bin are averaged over the number of elements within the bin. In doing so, and keeping in mind the definition of Ω_{nm}^λ , only values between 0 (no overlap between states) and 1 (wave functions are normalized) are possible. More details on the modulus overlap calculations are given in ref [26]. The results of our analysis are depicted in Fig. 4 (a) for electrons and in (b) for holes. Here, the zero of energy is taken as the valence band edge of the unstrained bulk GaN. For the sake of discussion, in the following we will use terms such as “conduction band” and “valence band”, even though this notation is strictly speaking not correct due to the presence of localized states. Starting with electrons, the bottom left corner of the figure corresponds to the “conduction band” edge which relates to electron states that are affected/localized by well width fluctuations; when approaching the top right corner of figure

1
2
3 4 (a) one is moving up higher in the “conduction band”. Overall, figure 4 (a) clearly shows
4
5 that there is large overlap between electron states with different energies. This means that
6
7 once carriers are excited in the “conduction band”, electrons can transfer easily from one
8
9 state to another. Consequently, when electrons are excited above the “conduction band” edge
10
11 they can easily be transferred to the localized states at the “band” edge. The situation is very
12
13 different for the holes, as depicted in figure 4 (b). Looking at the “valence band” edge (top
14
15 right corner of figure 4 (b)), we find strongly localized states, which have very little overlap
16
17 with states lower in energy, thus deeper in the “valence band”. Also, we observe that at lower
18
19 energies (bottom left corner) the overlaps between hole states are also large and comparable
20
21 to the numbers observed in our analysis of the electron states (figure 4 (a)).
22
23
24
25

26
27 Thus based on the theoretical results given above, the experimental data in figure 3 can be
28
29 explained in terms of a mobility edge. Overall it is important to note that the absolute
30
31 energies calculated here cannot be directly compared to the absolute energies obtained in the
32
33 experiment. This stems from the fact that for instance the well width and thus the PL peak
34
35 energy of the non-resonant PL are different between theory and experiment. However, as
36
37 discussed already above, the FWHM values in theory and experiment are similar, indicating
38
39 that the spread in electron and hole energies is realistically described by the theory. For the
40
41 present study of the mobility edge, this feature is key for the theory-experiment comparison.
42
43 Turning back to figure 3, excitation photon energies above the experimental mobility edge
44
45 (2.812 eV) results in the occupation of excited electron and hole states, assuming the primary
46
47 excitation process results in the creation of independent electrons and holes. Such a process
48
49 would correspond to carriers being excited in the states described by the upper right part of
50
51 figure 4 (a) (electrons) and bottom left corner of figure 4 (b) (holes). Carriers in these states
52
53 can, because of the strong wave function overlap between the excited electron and hole states,
54
55 scatter rapidly on the time scale of the PL recombination down to the localised electron and
56
57
58
59
60

1
2
3 hole states leading to the observed PL spectrum. When lowering the excitation energy, in
4 terms of electron states, one moves from the upper right to the lower left corner. Given that
5 the overlap between electron states with different energies is high and largely unaffected by
6 the change in energy, the electrons can still be transferred to the localized electron states.
7 Thus, we do not expect a significant contribution from the electron system to the mobility
8 edge observed in the experiment. The situation is drastically different for holes. In this case,
9 when lowering the excitation energy, in figure 4 (b) one moves from the bottom left region to
10 the upper right corner. In this case, and in contrast to the electrons, the wave function overlap
11 between the different hole states changes significantly with energy and carriers cannot be
12 easily transferred between different localised states. Thus excitation below the mobility edge
13 results in direct excitation of holes in localised states such that the carriers are not sufficiently
14 mobile at $T=12\text{K}$ to scatter to the other localised states. Hence as the excitation photon
15 energy is reduced the spectrum shifts accordingly as the energy of the states that are directly
16 populated also is progressively reduced. From this analysis we conclude that the mobility
17 edge is mainly determined by hole localisation.

38 **Conclusion**

39
40
41 In summary we have studied the form of the low temperature PL spectrum of a c-plane
42 InGaN/GaN QW structure as a function of excitation energy. For excitation photon energies
43 above 2.812 eV the spectra involve recombination of zero phonon and LO phonon
44 accompanied recombination of localised electrons and holes. For excitation photon energies
45 below 2.812 eV the form of the spectra are radically changed consisting mainly of LO and
46 acoustic phonon assisted recombination of resonantly excited localised states. The peak
47 energies of both these features shift to progressively lower photon energies as the excitation
48 photon energy is reduced.

1
2
3 This behaviour is consistent with the existence of a mobility edge whereby for excitation
4 below 2.812 eV localised carriers are not free to redistribute across the available localised
5 states. This interpretation is reinforced by a comparison with the results from an atomistic
6 tight-binding model. The results of these calculations show that the wave function overlap of
7 the lower energy localised hole states with other hole states is low whereas the electron-
8 electron wave function overlap is largely independent of energy. On this basis we attribute
9 the mobility edge to the strong localisation of the lowest lying holes.
10
11
12
13
14
15
16
17
18
19

20 **Acknowledgements**

21
22
23 This work was carried out with the support of the United Kingdom Engineering and Physical
24 Sciences Research Council under grant Nos. EP/M010589/1, EP/I012591/1, EP/M010627/1
25 and EP/H049533/1 and the Science Foundation Ireland (SFI) under Project No.
26 13/SIRG/2210. The data associated with the paper are openly available from
27 <http://dx.doi.org/10.17632/tdzkmm5gw3.2>
28
29
30
31
32
33
34
35
36
37
38
39
40
41
42
43
44
45
46
47
48
49
50
51
52
53
54
55
56
57
58
59
60

References

- [1] http://www.nobelprize.org/nobel_prizes/physics/laureates/2014/.
- [2] Galtrey M. J, Oliver R. A, Kappers M.J, Humphreys C. J, Clifton P, Larson D, Saxey D and Cerezo A 2008, *J. Appl. Phys.* **104**, 013524
- [3] Chichibu S, Wada K and S. Nakamura 1997 *Appl. Phys. Letts.*, **71**, 2346
- [4] Narukawa Y, Kawakami Y, Fujita S, S Fujita and Nakamura S 1997 *Phys. Rev B*, **55**, R1938
- [5] Smeeton T M, Kappers M J, Barnard J S, Vickers M E and Humphreys C J 2003 *Appl. Phys. Letts.*, **83**, 5419
- [6] Bennett S E, Saxey D W, Kappers M J, Barnard J S, Humphreys C J, Smith G D W and Oliver R A, 2011, *Appl. Phys. Lett.*, **99**, 21906
- [7] Tang F, Zhu T, Oehler F, Fu W Y, Griffiths J T, Massabuau F C-P, Kappers M J, Martin T L, Bagot P A J, Moody M P and Oliver R A, 2015 *Appl. Phys. Lett.*, **106**, 72104
- [8] Graham D M, Soltani-Vala A, Dawson P, Godfrey M J, Smeeton T M, Barnard J S, Kappers M J, Humphreys C J and Thrush E J, 2005 *J. Appl. Phys.*, **97**, 103508
- [9] Watson-Parris D, Godfrey M J, Dawson P, Oliver R A, Galtrey M J, Kappers M J and Humphreys C J 2011 *Phys. Rev. B*, **83**, 115321.
- [10] Schulz S, Caro M A, Coughlan C and O'Reilly E P 2015 *Phys. Rev. B*, **91**, 035439
- [11] Eliseev P G, Perlin P, Lee J and Osinski M 1997 *Appl. Phys. Letts.*, **71**, 569
- [12] Davidson J A, Dawson P, Wang T, Sugahara T, Orton J W and Sakai S 2000 *Semicon. Sci. Tech.*, **15**, 497
- [13] Morel A, Lefebvre P, Kalliakos S, Taliencio T, Bretagnon T and Gil B, 2003, *Phys. Rev. B*, **68**, 045331
- [14] Filoche M, Piccardo M, Wu Y-R, Li C-K, Weisbuch C and Mayboroda S, 2017, *Phys. Rev B*, **95**, 144204
- [15] Piccardo M, Li C-K, Wu Y-R, Speck J S, Bonef B, Farrell R M, Filoche M, Martinelli, Peretti J and Weisbuch C, 2017, *Phys. Rev. B* **95**, 144205
- [16] Brener I, Olszakier M, Cohen E, Ehrenfreund E, A Ron and Pfeiffer L 1992 *Phys Rev B*, **46**, 7927
- [17] Dawson P, Buckle P, Godfrey M J, Roepke W H and Halsall M 1997 *Sol Stat. Comms.*, **101**, 477

- 1
2
3 [18] Cohen E and Sturge M D 1982 Phys. Rev. B, **25**, 3828
4
5 [19] Permogorov S, Reznitkii A, Verbin S, Muller G O, Flogel P and Nikiforova M 1982
6 Phys Stat. Sol. B, 113, 589
7
8 [20] Satake A, Masumoto Y, Miyajima T, Asatsuma T, Nakamura F and Ikeda M 1998 Phys.
9 Rev. B, **57**, R2041
10
11 [21] Schmidt T J, Cho Y H, Bidnyk S, Song J J, Keller S, Mishra U K and Denbaars S P
12 1999 Proc. SPIE Conf. Physics and Simulation of Optoelectronic Devices VII, **3625**, 57
13
14 [22] Graham D M, Dawson P, Godfrey M J, Kappers M J and Humphreys C J 2006 Appl.
15 Phys. Letts., **89**, 211901
16
17 [23] Hylton N P, Dawson P, Kappers M J, McAleese C and Humphreys C J 2007 Phys. Rev.
18 B, **76**, 205403
19
20 [24] Mott N 1987 J. Phys C, **20**, 3075
21
22 [25] Schmidt T J, Cho Y H, G H Gainer, Song J J, Keller S, Mishra U K and DenBaars S P
23 1998 Appl. Phys. Letts., **73**, 560
24
25 [26] Tanner S P, Caro M A, O'Reilly E P and Schulz S 2016 RSC Advances, **6**, 64513
26
27 [27] Davies M J, Dawson P, Massabuau F C-P, Oehler F, Oliver R A, Kappers M J, Badcock
28 T J, and Humphreys C J, 2014, Phys. Status Solidi C **11**, 750
29
30 [28] Oliver R A, Massabuau F C-P, Kappers M J, Phillips W A, Thrush E J, Tartan C C,
31 Blenkhorn W E, Badcock T J, Dawson P, Hopkins M A, Allsopp D W E and Humphreys C J
32 2013, Appl. Phys. Letts., **103**, 141114
33
34
35
36
37
38
39
40
41
42
43
44
45
46
47
48
49
50
51
52
53
54
55
56
57
58
59
60

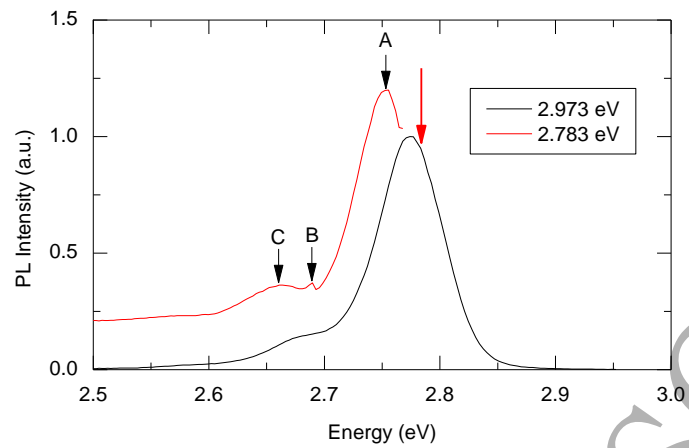


Figure 1. Photoluminescence spectra recorded at $T=12\text{K}$ for excitation photon energies of 2.973 eV and 2.783 eV as indicated. The energy of 2.783 eV is indicated by the red arrow. The nature of the transitions A, B and C are discussed in detail in the text.

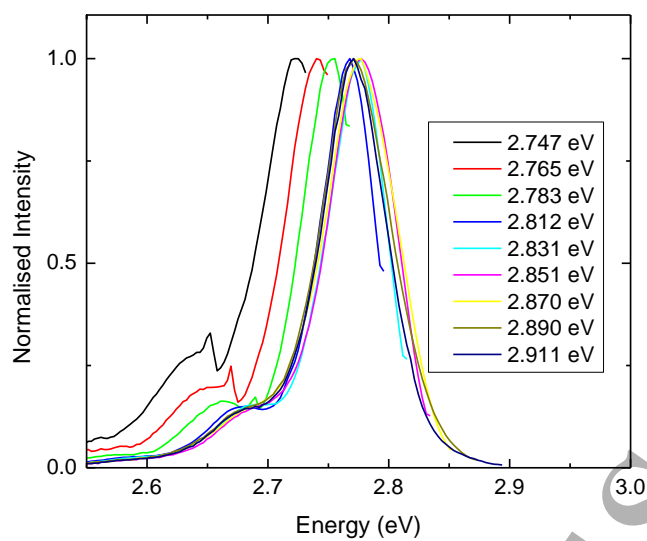


Figure 2. Photoluminescence spectra measured at $T=12\text{K}$ with the excitation photon energies indicated in the figure.

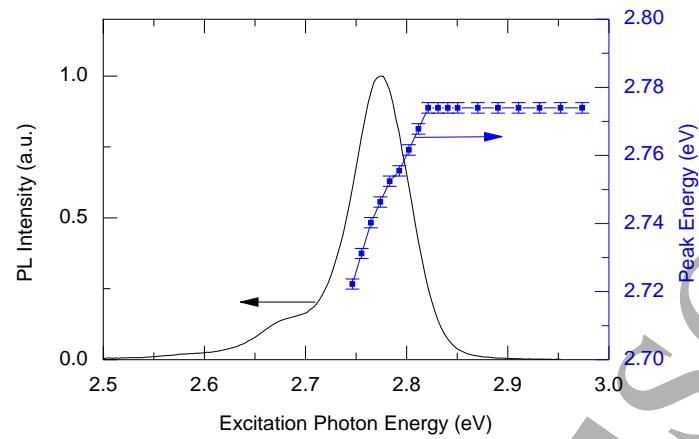


Figure 3. Photoluminescence spectrum (black) measured at $T=12\text{K}$ for excitation photon energy of 2.973 eV alongside a plot (blue circles) of the energy of peak photoluminescence intensity as a function of excitation energy.

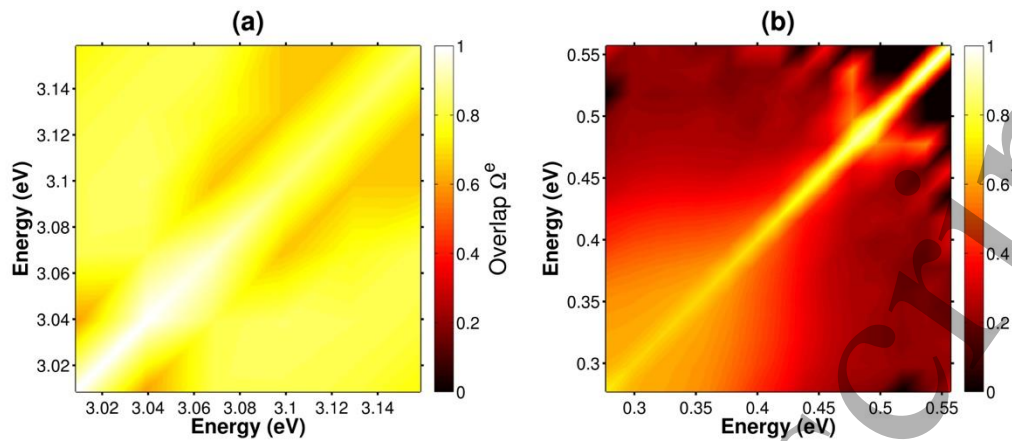


Figure 4 Modulus wave function overlap Ω for (a) electrons and (b) holes. The valence band edge of unstrained bulk GaN is taken as the zero of energy. Thus the QW “conduction band” edge corresponds to the lower left corner in (a), while the QW “valence band” edge is determined by the upper right corner in (b).